

**The Large Hadron electron Collider
as a bridge project for CERN
Documentation for the Physics Preparation Group
in response to Benchmark measurements / processes
Version 1.0**

March 31, 2025

Abstract

This document contains the responses from the LHeC community in answer to the benchmarking questions from the Physics Preparatory Group of the 2025-6 European Particle Physics Strategy Update. The benchmark document questions are reproduced in black, followed by answers, **in blue**. Where possible, it contains numbers and plots, together with references to supporting documents where further details can be found. In some places where work is still ongoing, it points to updates to follow later.

Version 1.0 of this document sits as part of the addendum document to the LHeC EPPSU submission. Subsequent updates, and further information arising from interactions with the relevant Working Groups as they prepare the briefing book, will be included in later versions. The latest version will be maintained at <http://epweb2.ph.bham.ac.uk/user/newman/ppg.lhec.latestversion.pdf>.

Contact person:

Paul R. Newman

School of Physics and Astronomy, University of Birmingham, B15 2TT, United Kingdom

E-mail: paul.newman@cern.ch

1 Higgs physics benchmarks

1.1 Precision of the measurement of the Higgs mass (and width, when a determination is possible)

Work in progress. Event numbers for decays into $\gamma\gamma$ or $4l$ are similar to those of ATLAS or CMS 2016 analyses, suggesting a similar uncertainty of ± 0.2 GeV.

On the other hand, from including LHeC PDFs+ α_s into LHC EW fits, a determination of the mass with uncertainty $\pm 8(10)$ GeV without (with) theory uncertainties is possible, see Fig. 1 [1], to be compared with $\pm 19(20)$ GeV from the EWK 2025 fit with no LHeC input.

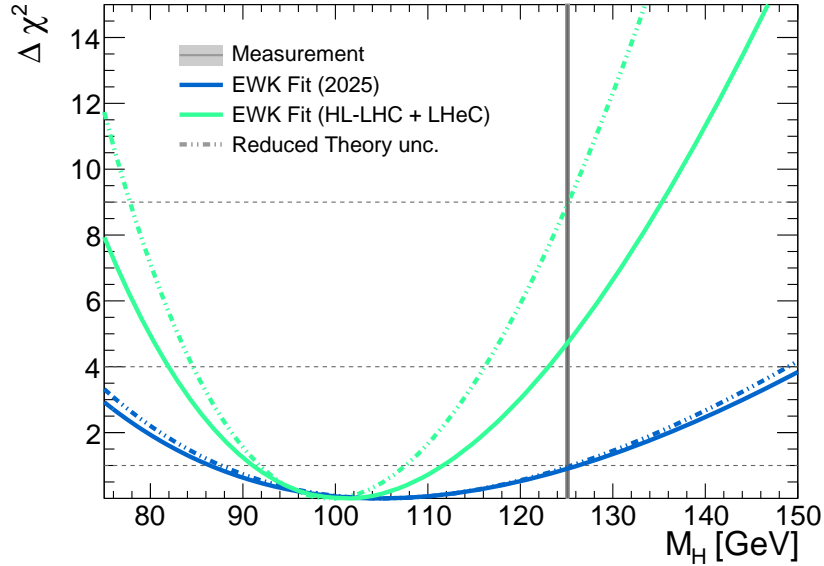


Figure 1: Present and future precision in the indirect determination of the Higgs-boson mass in the Standard Model.

1.2 Single Higgs couplings

- From Kappa fits, in combination with HL-LHC: All SM coupling modifiers AND non-SM Higgs decays
Fig. 2 [1] shows the incremental effect from the HL-LHC (light magenta), adding the effect of LHeC PDFs+ α_s (deep blue) to the inclusion of the LHeC determination of the couplings (green). Numbers can be read from the plots.
- From Kappa fits, in combination with HL-LHC: All SM coupling modifiers WITHOUT non-SM Higgs decays
Fig. 3 shows the incremental effect from the HL-LHC (light magenta), adding the effect of LHeC PDFs+ α_s (deep blue) to the inclusion of the LHeC determination of the couplings (green). Numbers can be read from the plots.
- From SMEFT fits: Baseline established with BSM / FlavorWGs. For the preparation of these studies we will need the projected uncertainties on the corresponding Higgs observables at each different energy and with correlations, when available.
Tables 1 and 2, from [8], show the signal strengths and the κ -values extracted from the LHeC alone.
- Shape of the Higgs potential. Precision on Higgs self-coupling
... from HH production or from single-Higgs measurement via SMEFT fit

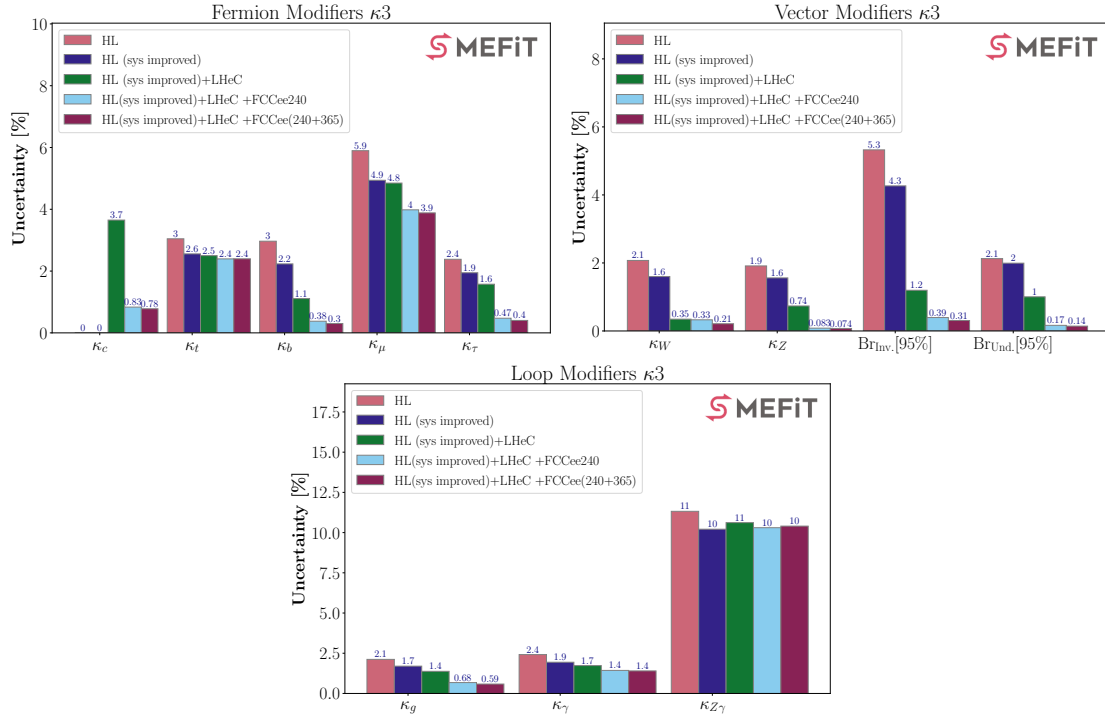


Figure 2: Relative uncertainty in the coupling modifiers obtained in the kappa-3 framework [2, 3], for different combinations of the HL-LHC, LHeC, and other future collider datasets. "HL-LHC(improved)" refers to the impact of reduced PDF+ α_s uncertainties in the HL-LHC measurements. These data are further combined with LHeC Higgs-boson measurements, and with either FCC-ee data at $\sqrt{s} = 240$ and 365 GeV. The fermion, vector, and loop modifiers are shown from top to bottom respectively. Since neither HL-LHC nor LHeC give direct access to the Higgs width, the condition $\kappa_V(\kappa_W, \kappa_Z) \leq 1$ is imposed on the fit and the uncertainty on these modifiers is defined as $1 - \kappa_V$ (68%). Results have been obtained with the SMEFIT framework [4–7]. From [1].

Setup	bb	$bb \oplus \text{Thy}$	WW	gg	$\tau\tau$	cc	ZZ	$\gamma\gamma$
LHeC NC	2.3	2.4	17	16	15	20	35	42
LHeC CC	0.80	0.94	6.2	5.8	5.2	7.1	12	15

Table 1: Summary of estimates on the experimental uncertainty of the signal strength μ , in per cent, for the seven most abundant Higgs decay channels, in charged and neutral currents for the LHeC, the HE-LHeC and the FCC-eh. The $b\bar{b}$ channel is the one which is most sensitive to theoretical uncertainties and for illustration is given two corresponding columns.

Coupling κ for decay $H \rightarrow$	$b\bar{b}$	WW	gg	$\tau\tau$	$c\bar{c}$	ZZ	$\gamma\gamma$
Relative uncertainty $\delta\kappa$ (%)	1.9	0.70	3.5	3.1	3.8	1.2	6.8

Table 2: Summary of uncertainties of Higgs couplings from ep for the seven most abundant decay channels.

$-2.74 < \kappa_\lambda < 5.28$ at 95% C.L. from single Higgs production (Fig. 7 in [9]). More refined heavy-flavour tagging would improve this result. These limits compete with those from single-top production at the HL-LHC, not with those coming from di-Higgs production.

The LHeC can probe the CP structure of the Higgs Yukawa coupling [10], for instance, via $pe^- \rightarrow \bar{t}h\nu_e$. Assuming a SM-like top-Yukawa coupling, the coupling magnitude could be measured with 17% accuracy at the LHeC using 1 ab^{-1} of integrated luminosity [10].

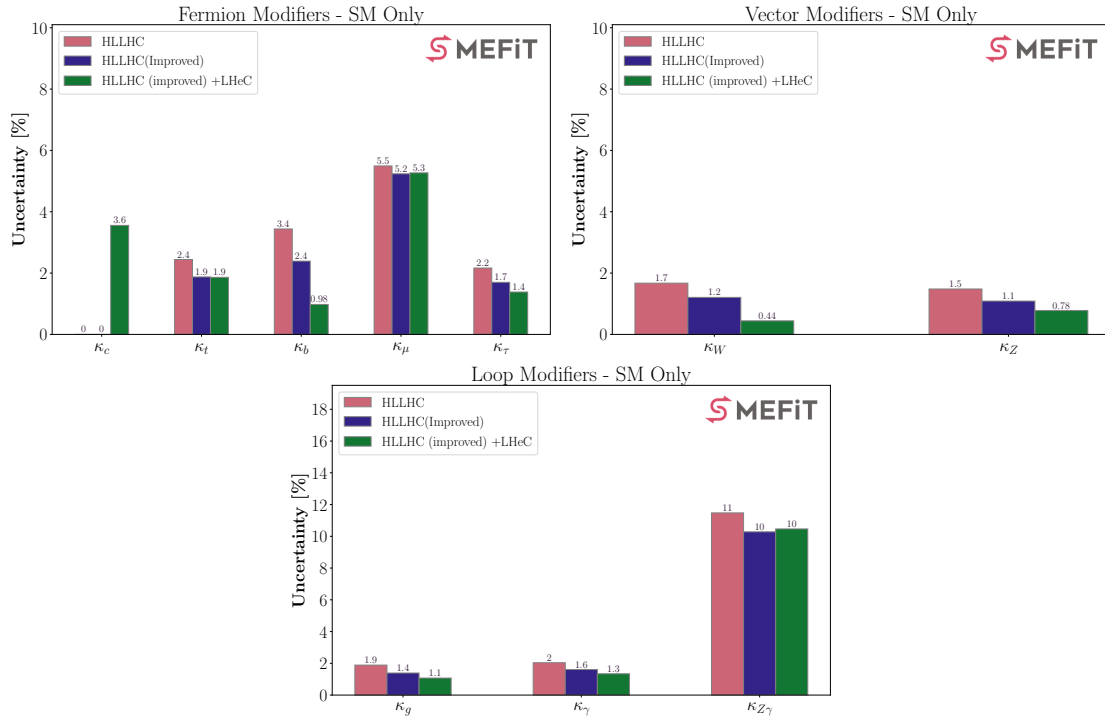


Figure 3: Relative uncertainty in the coupling modifiers obtained in the SM-only framework [2,3], for different combinations of the HL-LHC and LHeC. "HL-LHC(improved)" refers to the impact of reduced PDF+ α_s uncertainties in the HL-LHC measurements. The fermion, vector, and loop modifiers are shown from top left, top right and bottom respectively. Since neither HL-LHC nor LHeC give direct access to the Higgs width, the condition $\kappa_V(\kappa_W, \kappa_Z) \leq 1$ is imposed on the fit and the uncertainty on these modifiers is defined as $1 - \kappa_V$ (68%). Results have been obtained with the SMEFIT framework [4–7].

2 Electroweak physics benchmarks

2.1 Precision Electroweak measurements

2.1.1 Projected uncertainties on Electroweak precision observables (without imposing any assumption about fermion universality)

- On-shell Z measurements: M_Z , Γ_Z , σ_{had}^0 , R_f , Asymmetries (A_{FB}^f , A_f), etc. with $f = e, \mu, \tau, b, c, s \dots$
 M_Z : ± 13 MeV standalone [8]; < 2 MeV in combination with the HL-LHC [1]. Further work in progress; the expected yields are:
 - Z in NC: $\sigma = 0.94$ pb \rightarrow about 10^6 on-shell Z events.
 - Z in CC: $\sigma = 0.83$ pb \rightarrow about $0.8 \cdot 10^6$ on-shell Z events.
- On-shell W measurements: M_W , Γ_W , BR($W \rightarrow e\nu, \mu\nu, \tau\nu$) ...
 M_W : ± 10 MeV standalone [8]; ± 3 MeV in combination with the HL-LHC [1]. Further work in progress; the expected yields are:
 - W in NC: $\sigma = 2.6$ pb \rightarrow about $2.6 \cdot 10^6$ on-shell W events.
 - W in CC: $\sigma = 5.6$ pb \rightarrow about $5.6 \cdot 10^6$ on-shell W events.
 - $\gamma\gamma \rightarrow WW$: $\sigma = 100$ fb \rightarrow about 10^5 WW events.
- Other Observables / Pseudo-Observables. e.g. definitions and expected precision in observables used for determination of anomalous triple gauge couplings (aTGC) from diBoson production.
 $\sin^2 \theta$: ± 0.00022 standalone [8]; ± 0.00008 in combination with the HL-LHC [1]. Also its running with scale, Fig. 4 [1].

g_A^u (axial up-Z coupling from t channel Z exchange): 0.0035 ([8, 11]).

g_A^d : 0.0083 ([8, 11]).

g_V^u : 0.0028 ([8, 11], Fig. 5 [1]).

g_V^d : 0.0067 ([8, 11], Fig. 5 [1]).

Anomalous triple gauge couplings: limits obtained from direct production of W, Z, γ ([8] section 5.2.2, see Fig. 6).

Other observables are:

- Anomalous high-order corrections in CC vertices $\rho'_{CC,eq}$ and $\rho'_{CC,e\bar{q}}$ [8, 11], parameters not yet mapped to SMEFT, shown in Fig. 7.
- Scale-dependent measurements of ρ_{NC} , ρ_{CC} : work in progress.

2.1.2 EW couplings: sensitivity to BSM in Z and W couplings to SM fermions.

From SMEFT fits: Same setup used in “Single Higgs Couplings”

Limits on dimension-6 operators are shown in Fig. 8 [1].

See also Figs. 6 and 7 and comments above.

2.2 Other probes of Electroweak symmetry breaking / Multi-Boson processes

e.g. Longitudinal Vector Boson Scattering (VBS): Same-sign VBS at Hadron colliders, VBF/VBS at lepton colliders.

Work in progress.

Assuming the integrated luminosity of 1 ab^{-1} , about 100000 W^\pm boson pairs will be produced at the LHeC via photon-photon fusion [1, 21].

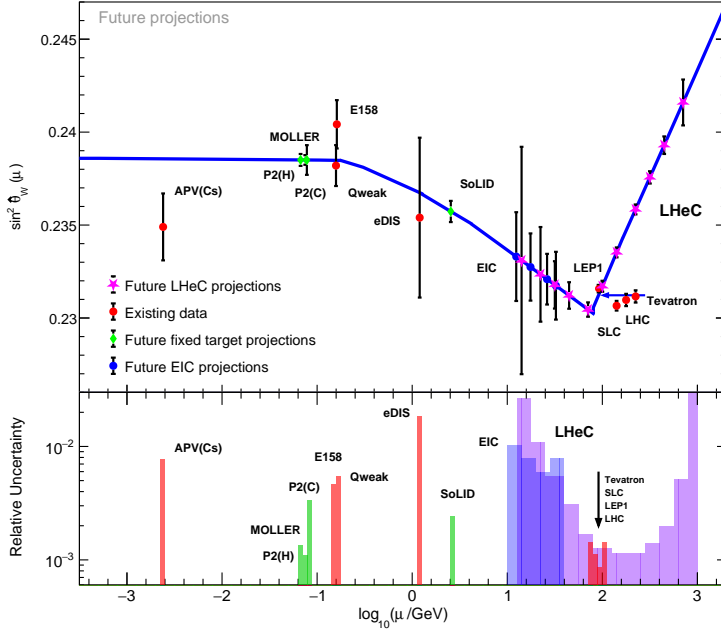


Figure 4: Present and future measurements of the running of the weak mixing angle in the $\overline{\text{MS}}$ scheme and prospected uncertainties as a function of the scale μ . (Thanks to: J. Erler, R. Ferro-Hernandez and X. Zheng; updated from [12, 13], including recent projections from the Electron Ion Collider (EIC) [14], P2(C) at MESA [15] and the LHeC [11]). The red markers and red uncertainties show present measurements and their relative uncertainties, respectively, and further data points display future projections as indicated.

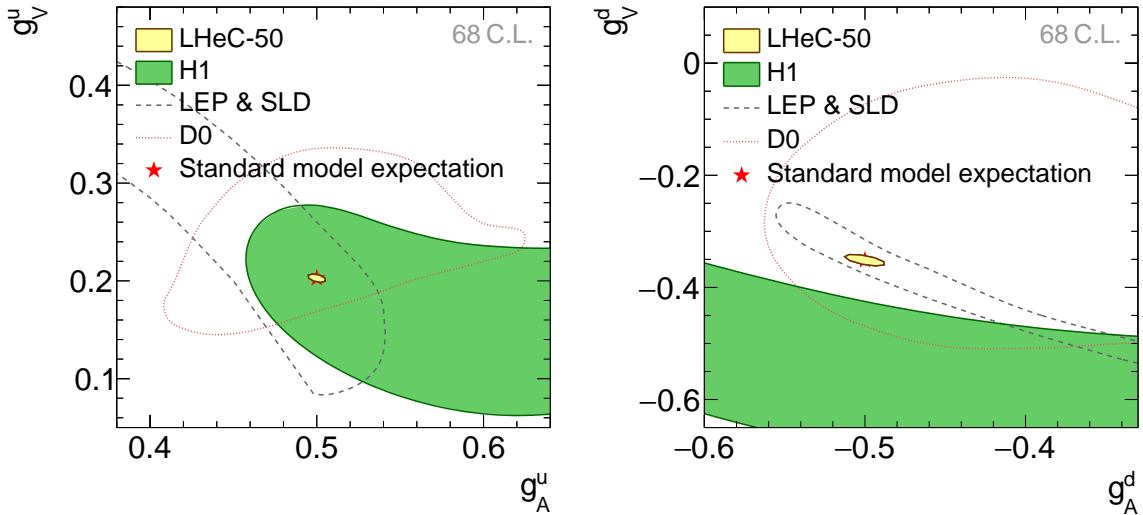


Figure 5: Weak NC vector and axial-vector couplings of u -type (left) and d -type quarks (right) at 68% confidence level (CL) for simulated LHeC data with $E_e = 50$ GeV. The LHeC expectation is compared with results from the combined LEP+SLD experiments [16], a single measurement from D0 [17] and one from H1 [18]. The standard model expectations are displayed by a red star, partially hidden by the LHeC prospects.

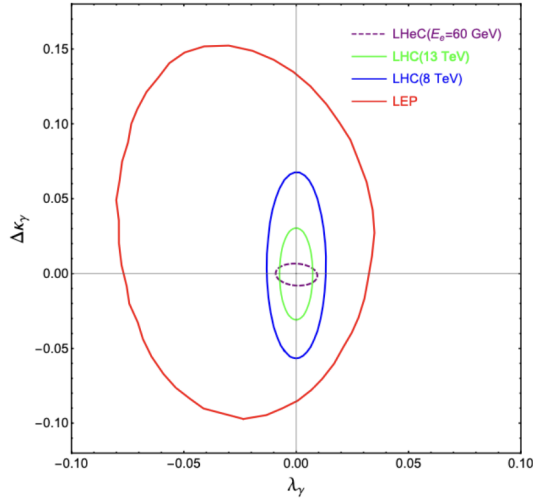


Figure 6: Anomalous triple gauge coupling summary [8].

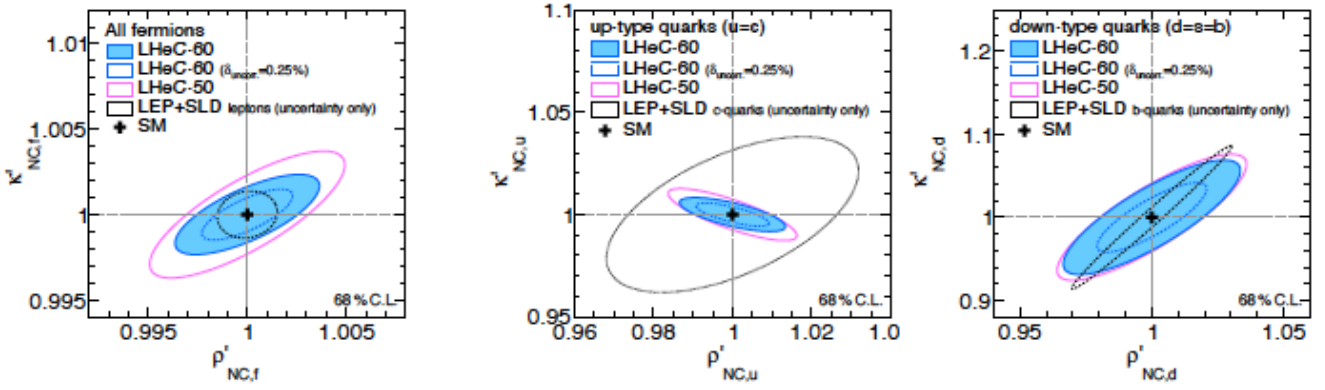


Figure 7: Anomalous weak neutral couplings [8, 11].

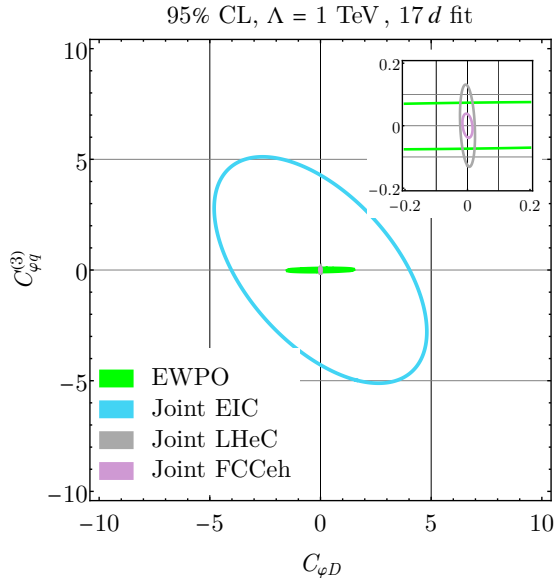


Figure 8: Marginalized 95% CL ellipses in the two-parameter fits of SMEFT dimension-6 operators $C_{\phi D}$ and $C_{\phi q}^{(3)}$ (right) at UV cut-off scale, $\Lambda = 1$ TeV [19]. Shown are joint EIC, LHeC, and FCC-eh fits, as well as the EWPO fit adapted from [20].

3 Top physics benchmarks

3.1 Top-quark mass precision

In progress. ± 1.4 GeV in standalone mode [8]; < 200 MeV in combination with the HL-LHC [1].

3.2 Top-quark properties from SMEFT fits

- Top-quark EW couplings (Ztt , Wtb)

Wtb to 1%, and anomalous coupling determination given in Table 3 [1, 8]. $|V_{ts}|$ limit down to 0.04, see Fig. 9 where the individual limits for three different signals are provided [8]. The nominal LHeC integrated luminosity is 1 ab^{-1} . For anomalous MDM and EDM of the top quark, LHeC gives $-0.13 < \kappa < 0.18$, and $|\tilde{\kappa}| < 0.38$, respectively, at 2σ C.L. [22].

Anomalous Wtb Coupling	f_R^1	f_L^2	f_R^2
LHeC, 1000 fb^{-1} ($\mathcal{R}e$)	[-0.13,0.14]	[-0.05,0.04]	[-0.10,0.09]

Table 3: Expected limits at 95% CL on anomalous right-handed vector (f_R^1), left-handed tensor (f_L^2) and right-handed tensor (f_R^2) Wtb couplings at the LHeC [8].

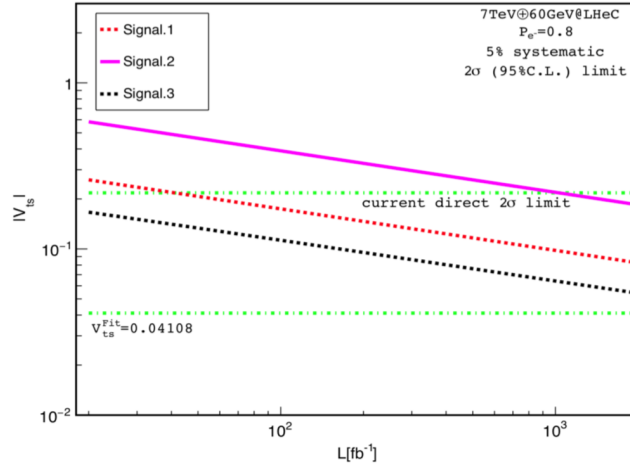


Figure 9: Expected sensitivities on $|V_{ts}|$ exploring three different signal scenarios (Signal 1: $pe^- \rightarrow \nu_e \bar{t} \rightarrow \nu_e W^- \bar{b} \rightarrow \nu_e \ell^- \nu_\ell \bar{b}$; Signal 2: $pe^- \rightarrow \nu_e W^- b \rightarrow \nu_e \ell^- \nu_\ell b$; Signal 3: $pe^- \rightarrow \nu_e \bar{t} \rightarrow \nu_e W^- j \rightarrow \nu_e \ell^- \nu_\ell j$) [23], as a function of the integrated luminosity.

- Top-quark Yukawa coupling

As mentioned in section 1.2 above, the LHeC can probe the CP structure of the Higgs Yukawa coupling [10], for instance, via $pe^- \rightarrow \bar{t} h \nu_e$. Assuming a SM-like top-Yukawa coupling, the coupling magnitude could be measured with 17% accuracy at the LHeC using 1 ab^{-1} of integrated luminosity [10].

- Other interactions entering in Top processes, depending on assumptions chosen in SMEFT fit, e.g. four-fermion interactions, Top-dipole operators

Limits of $BR(t \rightarrow \gamma q) < 1 \cdot 10^{-5}$ and $BR(t \rightarrow Zq) < 4 \cdot 10^{-5}$ at 2σ C.L. [8]. $|V_{td}| < 1.8 \times |V_{td}^{\text{PDG}}|$ [24].

4 Strong Interactions

4.1 Precision QCD

4.1.1 $\alpha_S(m_Z)$ and its Q^2 dependence

At the Z pole, 0.00022 from inclusive DIS fits, 0.00016 with inclusive + jets (experimental uncertainties only) [1]. The running is also measured [1], see Fig. 10.

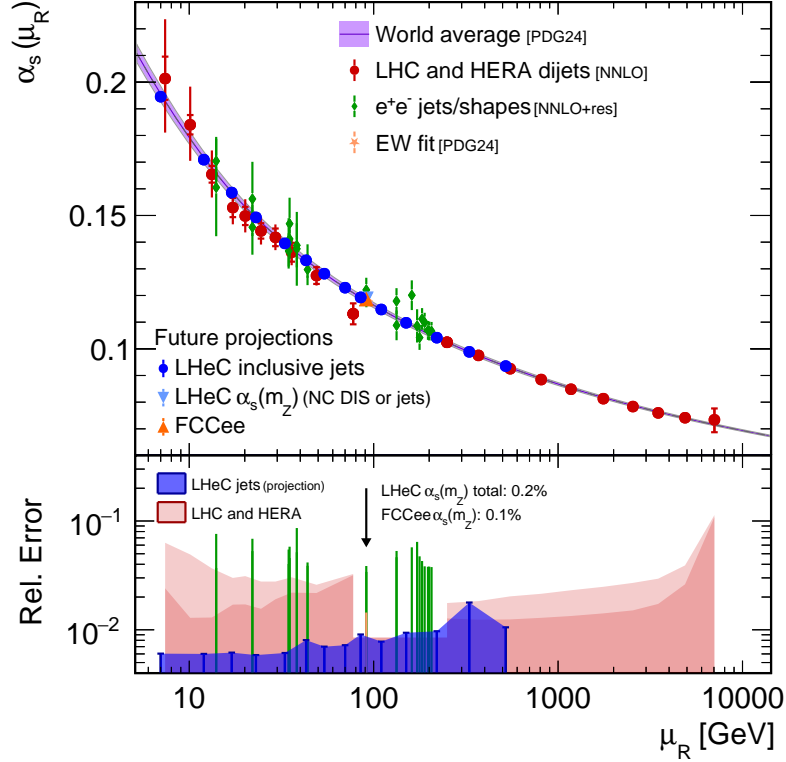


Figure 10: Expected measurement of $\alpha_s(\mu_R)$ [8] and corresponding relative uncertainties at the LHeC compared with presently available measurements [25, 26], predictions [27] and the world average value. The lower panel displays relative uncertainties on $\alpha_s(\mu_R)$, where light-shaded areas show experimental plus theoretical uncertainties and dark shaded areas experimental uncertainties only.

4.1.2 Strong interaction effects for precision measurements of top and W masses

... ep collisions: m_t from heavy-quark DIS (top-quark structure function measurements); m_W from inclusive DIS (charged-current structure function measurements);

Effects of the inclusion of LHeC information on PDFs and α_s are given in Table 4, while those on the uncertainties in the Higgs cross section through gluon-gluon fusion are given in Table 5 [1].

Parameter	Unit	Value	Uncertainty		
			Present	HL-LHC	HL-LHC+LHeC
m_Z	MeV	91187.6	2.1	< 2	< 2
m_W	MeV	80369.2	13.3	5–6	3
m_{top}	GeV	172.57	0.29	< 0.2	< 0.2

Table 4: Present and future precision in the determination of selected parameters of the electroweak and strong interactions.

4.2 Inner structure of protons and nuclei

4.2.1 Longitudinal and transverse proton PDF(x, Q^2)

...Parton flavours, Bjorken- x and Q^2 ranges for which new constraints and reduction of uncertainties are expected

\sqrt{s} [TeV]	$\sigma_{gg \rightarrow H}$ [pb]	TH uncertainty		PDF+ α_S uncertainty			Total		
		Ref.	S2	Ref.	S2	S2+LHeC	Ref.	S2	S2+LHeC
14	54.7	3.9%	2.0%	3.2%	1.6%	0.5%	5.1%	2.6%	2.0%
27	146.6	4.0%	2.0%	3.3%	1.7%	0.6%	5.2%	2.6%	2.1%
100	804.4	4.2%	2.1%	3.7%	1.9%	0.7%	5.6%	2.8%	2.2%

Table 5: Gluon-fusion Higgs cross-sections at $\sqrt{s}=14, 27$ and 100 TeV. The reference values and uncertainties are taken from [28] and symmetrized. The improved theoretical predictions are from [29–32].

See Figs. 11 and 12 [1], and many more in Sections 3.3 and 3.4 in [8].

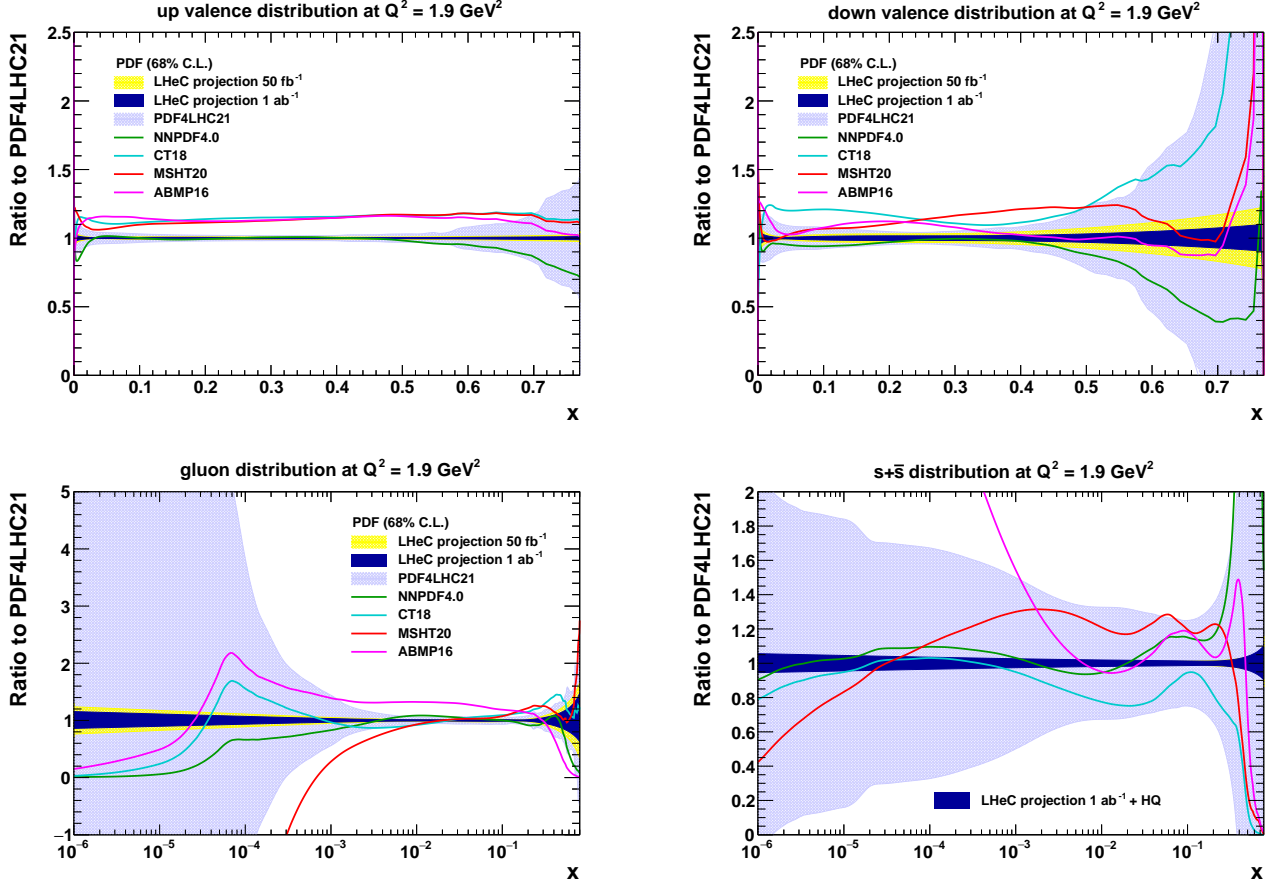


Figure 11: Expected precision for the determination of parton density functions, expressed as a ratio to that of PDF4LHC21 [33], as a function of x at $Q^2 = 1.9 \text{ GeV}^2$: u_v (top left), d_v (top right), g (bottom left) and s (bottom right). LHeC results at next-to-next-to-leading order (NNLO) for integrated luminosities of 50 fb^{-1} and 1 ab^{-1} are shown with uncertainty bands together with central values of ABMP16 [34], CT18 [35], MSHT20 [36] and NNPDF4.0 [37]. Small irregularities are due to those in the baseline set PDF4LHC21.

... Longitudinal and transverse nuclear PDF(x, Q^2); same as above;
 Sections 6.2 and 6.3 in [8].

4.3 Hot and dense QCD

- QGP transport coefficients (heavy quarks, jets): expected precision for observables that constrain the transport coefficients that characterise parton energy loss and heavy-quark interactions in the QGP;

Work in progress. Fig. 13 shows the expected precision on the ratio of jet cross sections in ep and ePb at the LHeC. The data then probes directly, and only, the nuclear modification terms in the nPDFs or, if fixed from inclusive data, check factorisation or indicate other cold nuclear matter effects like jet quenching.

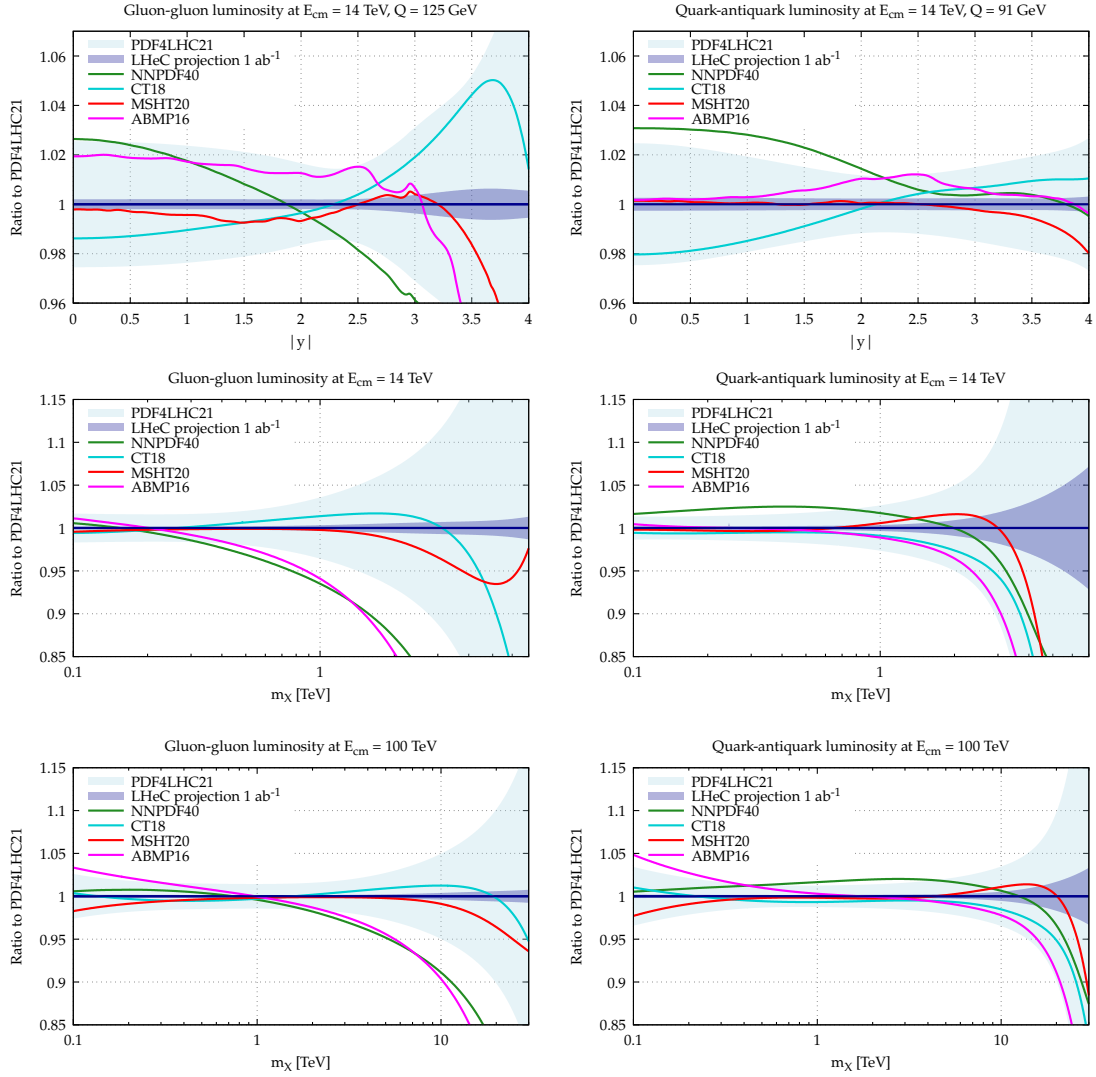


Figure 12: Parton-parton luminosities as a function of rapidity (gg on the left, $q\bar{q}$ on the right), at $\sqrt{s} = 14$ eV (top), and as a function invariant mass at $\sqrt{s} = 14$ (middle) and 100 TeV (bottom), normalized to PDF4LHC21 [33]. LHeC results at NNLO are shown with uncertainty bands together with central values of ABMP16 [34], CT18 [35], MSHT20 [36] and NNPDF4.0 [37].

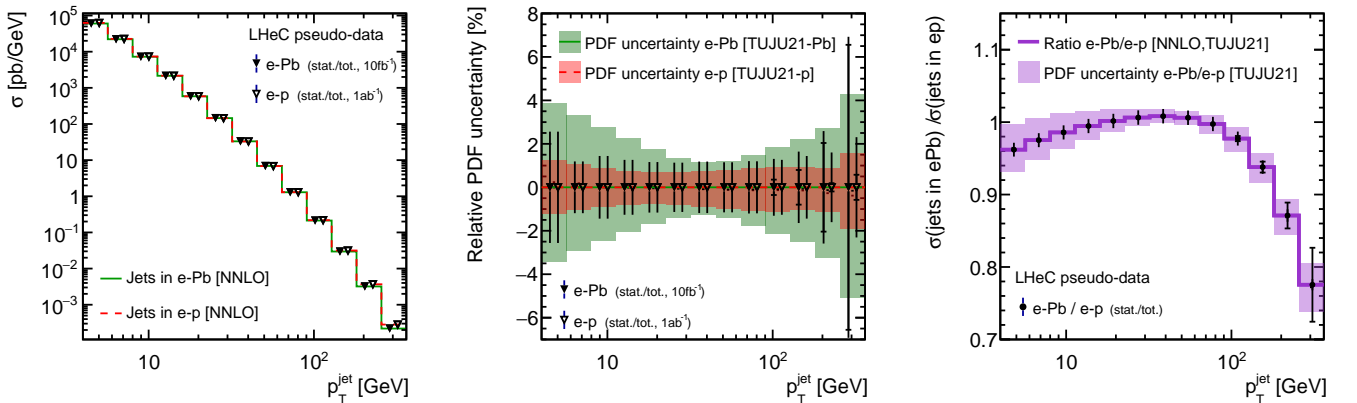


Figure 13: Single jet cross sections in ep and ePb (left), their PDF uncertainties (middle), and their ratio (right), at NNLO, using proton and nuclear PDFs from [38].

4.4 QCD connections with hadronic, nuclear and astro(particle) physics

- Constraints on nature of exotic hadrons from spectroscopy and h-h correlations; expected measurements that can help understanding the structure of exotic heavy-flavour hadrons (e.g. compact tetraquark vs.

hadron molecule), including direct measurements of yields, resonant states, kinematic distributions in different collision systems, and hadron-hadron momentum correlation functions that have sensitivity to bound states

No work done so far, but similar possibilities to those at the EIC for spectroscopy would exist [39].

- Precision on anti-nuclei production and absorption relevant for cosmic-ray physics: production of light anti-nuclei (e.g. \bar{p} , \bar{d} , ${}^3\bar{H}e$) that constrain production processes and kinematic distributions in primary cosmic-ray interactions; annihilation cross sections for anti-nuclei on nuclei, relevant for the propagation of cosmic anti-nuclei in space (e.g. from Dark Matter decays);

Small- x PDFs required to constrain forward charm production, neutrino-nucleon cross sections and tau energy loss for earth-skimming neutrinos, as discussed in section 4.2.6 in [40] and section 3.3 in [8].

5 Flavour physics

- τ lifetime, $\text{BR}(\tau \rightarrow \mu\nu\nu)$ and $\text{BR}(\tau \rightarrow e\nu\nu)$ (τ universality tests)

Fully exclusive two-photon production of tau-lepton pairs has a large cross section of almost 50 pb at the LHeC, for pair invariant masses above 10 GeV [21]. This leads to an excellent sensitivity to the τ anomalous magnetic moment a_τ . Already with an integrated ep luminosity of 100 fb^{-1} , the expected LHeC sensitivity is an order of magnitude better than that achieved at the LHC. As a result, for the first time the experimental uncertainties will be better than the higher order corrections to the τ magnetic moment in the SM.

- CKM elements from W decays

As indicated in section 3.2 above, $|V_{tb}|$ can be determined with 1% accuracy, and $|V_{ts}| < 0.04$, at 95% C.L.

6 BSM physics

Specific questions and corresponding new physics scenarios that can be constrained or discovered at present and future experiments, through multi-pronged approaches, combining collider data with other experiments and observations at different scales.

- New gauge forces (Z' , W' ...): U(1)-Y-universal, $U(1)_{B-L}$ (universal and 3rd gen), HVT $SU(2)_L$ custodial, HVT Right-handed

Work in progress.

- Compositeness (indirectly from EFT fits): Scenario discussed in 1905.03764 + 4q, 2q-2l

Work in progress. As shown in Table 9.6 in [8] (reproduced below), the use of PDFs and α_s from the LHeC extends the reach for contact interactions to larger scales than at the HL-LHC by $> 35\%$.

Model	ATLAS (Ref. [702])	HL-LHC	
	$\mathcal{L} = 36 \text{ fb}^{-1}$ (CT14nnlo)	$\mathcal{L} = 3 \text{ ab}^{-1}$ (CT14nnlo)	$\mathcal{L} = 3 \text{ ab}^{-1}$ (LHeC)
LL (constr.)	28 TeV	58 TeV	96 TeV
LL (destr.)	21 TeV	49 TeV	77 TeV
RR (constr.)	26 TeV	58 TeV	84 TeV
RR (destr.)	22 TeV	61 TeV	75 TeV
LR (constr.)	26 TeV	49 TeV	81 TeV
LR (destr.)	22 TeV	45 TeV	62 TeV

- Extension of the minimal real scalar sector giving 1st order EW phase transition and possibly stability: scenario discussed in e.g. 2303.03612

Work in progress.

- Minimal dark matter (WIMP) global: see e.g. 2107.09688

Work in progress. The LHeC could be sensitive to low mass DM candidates in possibly modified scenarios through disappearing track signature, similar to what is presented for Higgsino scenarios in Fig. 8.6 in [8].

- Flavor (together with flavor group): scalar and vector leptoquarks with third generation specificities

Work in progress. Leptoquark states at low energy could be characterised at the LHeC, see section 8.6.1 in [8].

- SUSY (direct only collider, global or with specific assumptions): see Briefing Book 2020

See section 8.3 in [8].

- Portals (dark photon, dark higgs, HNLs, axions, ALPs): see Briefing Book 2020

Constraints can be placed on ALPs, see Fig. 14 [1], and also section 8.4.4 in [8].

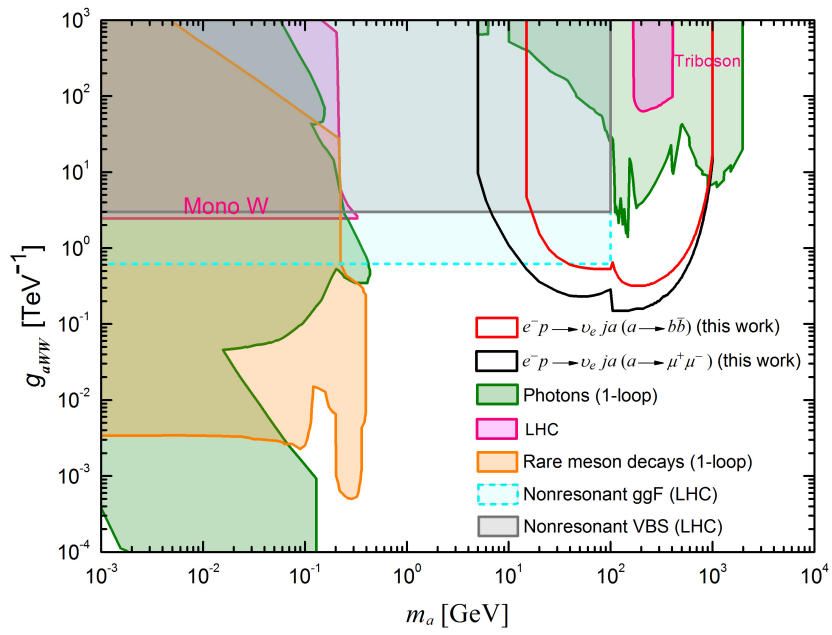


Figure 14: Projected 2σ sensitivity limits on the coupling of ALP to W^\pm bosons at the LHeC [41] in comparison with other current excluded regions.

7 Neutrinos and cosmic messengers

Heavy sterile neutrinos can be constrained at the LHeC through displaced vertices and trijet signals, see Fig. 15 [1, 8].

Also and as stated in section 4.4 above, small- x PDFs are required to constrain forward charm production, neutrino-nucleon cross sections and tau energy loss for earth-skimming neutrinos, section 4.2.6 in [40] and section 3.3 in [8].

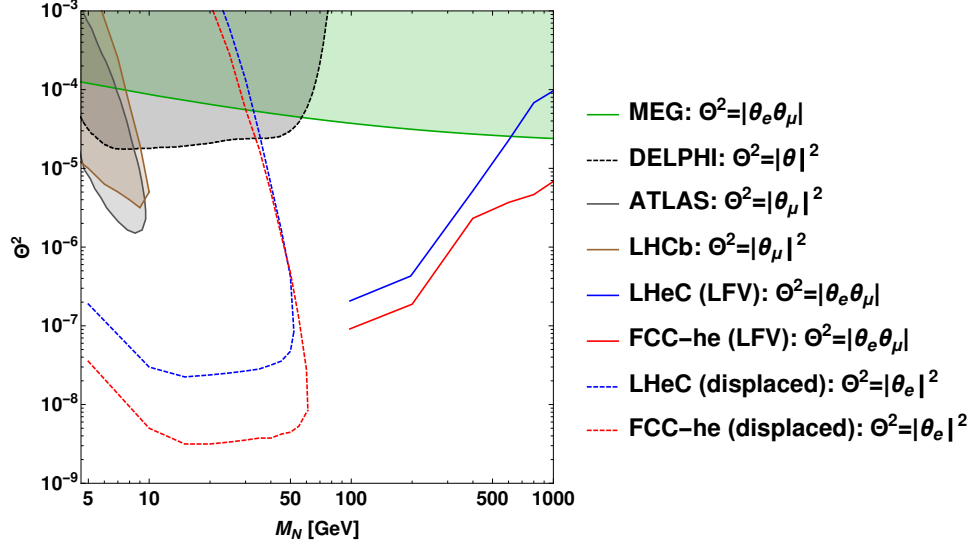


Figure 15: Sensitivity of the LFV lepton-trijet searches (at 95% C.L.) and the displaced vertex searches (at 95% C.L.) [42] compared to the current exclusion limits from ATLAS [43], LHCb [44], LEP [45], and MEG [46]. The sensitivity of the lepton-trijet searches at ep colliders can be generalized to its full θ_α -dependence by replacing $|\theta_e \theta_\mu|$ with $2|\theta_e|^2 |\theta_\mu|^2 / |\theta|^2$.

8 Dark Matter and Dark Sector

The models, broken down by mass range, are

- Light DM: ALPs, Z' (Dark Photon), Freeze-In Dark Matter
[Results on ALPs are given in Section 6 above.](#)
- Heavy DM: Wino & Higgsino, Higgs Portal, Scalar and Pseudoscalar mediator simplified models (O1 and velocity-dependent)
[LHeC results on Wino/Higgsino sensitivity are commented in section 6 above, also in section 8.3 in \[8\].](#)

9 Accelerator technologies

Please see separate LHeC document on [Technical Input for Large-Scale Projects](#).

10 Detector instrumentation

Whilst the instrumentation technology choices for the LHeC are not yet set in stone, a detailed description of a possible design is provided in the CDR update [8], where the emphasis was placed on providing a solution that could be built already now. In the following, we give answers based on the CDR update version, where further details can be found. We note in passing that more ambitious choices with higher levels of performance and correspondingly extended physics capabilities might also be considered if the project moves forwards towards realisation.

The PPG requests that the following information and/or specifications (instead of “benchmarks”) be given for each proposal submitted to the ESPPU dealing with detector instrumentation. Each project, be it on individual detection technologies or on devices/systems (tracker, calorimeter,...), should address the following points:

- What are the key performance indicators (KPIs) of your technology and which performance does your technology achieve in terms of these KPIs?
 - Central tracker: $\sigma(p_T) < 2\%$ for $p_T = 100$ GeV and $|\eta| < 3.5$. $\sigma(p_T) < 10\%$ for $|\eta| < 4.5$. $\sigma(d_0) < 20\mu\text{m}$ for $p_T > 10$ GeV and $|\eta| < 3$.
 - Electromagnetic Calorimeter: $\sigma(E)/E \lesssim 10\%/\sqrt{E} + 2\%$ except for forward plug, $\sigma(E)/E \lesssim 15\%/\sqrt{E} + 2\%$, for $\eta > 2.5$; position resolution for EM clusters < 1 mm .
 - Hadronic Calorimeter: $\sigma(E)/E \lesssim 50\%/\sqrt{E} + 5\%$.
 - Muon detector: at least two stations of trackers immersed in return yoke, each with $< 100\mu\text{m}$ resolution.
- What is the current technology readiness level (TRL, in the spirit of ISO norm 16290:2013) of your technology? How do you expect the technology to scale from lab prototypes to full detector systems (concerning mechanical integration, powering, cooling, readout)? If applicable: please start from the assessment by the ECFA detector roadmap and report updates.
 - Central tracker: the baseline is HV-CMOS technology, at TRL9 (ALICE ITS2); the innermost layers with bent silicon are at TRL6 (working prototype of ALICE ITS3); a further option to place the innermost layers and/or innermost part of the forward wheels inside the vacuum (LHCb VELO for LHC run3) is at TRL3 (synchrotron radiation tolerance, mechanical structure etc. still under investigation).
 - Calorimeter: Barrel EM with Lar: TRL9 (ATLAS EM); alternative EM or Hadcal based on scintillator sandwich: TRL6 (CALICE full prototype); endcap Si/Pb or W sandwich: TRL6 (SiD prototype, ALICE FoCal prototype etc.)
 - Muon: TRL9 (ATLAS and CMS muon systems)
- What are status and time scales for the project? At which point in time have you achieved or do you intend to achieve: proof of principle, concept validation (by full simulation), initial prototype, lab test, beam test, “slice” of full system, full system? Cover hardware, software and firmware aspects.

A very tentative timeline is supplied below which achieves full operation from 2044, three years after the HL-LHC end-point. We have arrived at this schedule on the assumption that it takes about 10 years from TDR to full construction of the detector if resource is available, of which the first four years are for final prototype, the remainder for production. We have allowed six years from the current time to the first prototypes, which factors in the heavy overlap in personnel with people working on the HL-LHC upgrades, operations and physics exploitation and the EIC construction.

- Concept validation with full simulation: ongoing in 2025
- Initial prototype with lab test: by 2031
- Initial prototype with beam test: by 2033
- Final prototype with slice of the full system: by 2035

- Detector construction: 2035 – 2041
- Installation and commissioning: 2042 – 2043
- Full detector in operation : from 2044
- Which DRD collaboration(s) are the most relevant to your technology? Is your technology already covered in one or more of them?
 - Central tracker: DRD3 Solid State Detectors – DRDT3.1 (CMOS sensors) and DRDT 3.4 (3D integration) – DRD WG 1 and WP1 (Monolithic silicon technologies)
 - Calorimeter: DRD6 – DRDT6.1 (rad-hard EM), DRDT 6.2 (high granular Calo) and DRDT 6.3 (extreme radiation - for forward rapidities and zero-degree calorimeter) – WP1 (sandwich calorimeters with fully embedded electronics), WP2 (liquified noble gas calorimeters), WP4 (electronics and DAQ)
 - Muon: DRD1 Gaseous Detectors – DRDT 1.1 (time, spatial resolution + longevity), DRDT 1.3 (environmental friendly gas) – WP1 (Trackers and Hodoscopes) and WP3 (Straw and Drift Tube Chambers) – WG3 (gas and materials) and other WGs
- What is the environmental impact of your technology/device/system and which measures are taken to reduce it?

The LHeC project has sustainability at its heart through its promotion of the development of Energy Recovery Linacs and energy-efficient superconducting RF. Similar considerations for the proposed detector lead to the immediate conclusion that any gaseous detectors have to use environmentally friendly gases. In the present design, this relates only to the muon detector, where the performance requirements are relatively modest, such that it should be easily possible to choose a technology with little-or-no environmental impact.

Since the currently proposed plan for the LHeC is to begin operations a few years after the end of the HL-LHC, the possibility naturally arises of limiting both financial and environmental costs by re-using LHC infrastructure and components. Detailed investigations have yet to be performed, but suggestions include recycling the ALICE3 tracker, or the CMS or ATLAS calorimeter solenoids, muons detectors or cryo plants, depending on which IP is finally chosen.

11 Computing

A detailed plan for data acquisition and off-line computing has yet to be developed for the LHeC. However, it is possible to make some estimates based for example on comparisons of even rates and sizes with LHC experiments and plans for the EIC.

It is assumed that the experiment will have a streaming readout without any hardware triggering, which is possible due to the relatively modest event rate. Depending on costs and available resources, all events could be permanently recorded, at least in some compressed form, or else prescaling schemes could be applied to the lowest $Q^2 \rightarrow 0$ 'photoproduction' events, or even some low Q^2 electroproduction, after a first off-line processing.

Our assumption in arriving at the estimates below is that we have a streaming readout, but permanently save only 10kHz, independently of the delivered luminosity. This would allow us to retain all events with $Q^2 > 10 \text{ GeV}^2$ at a luminosity of $10^{33} \text{ cm}^{-2}\text{s}^{-1}$, with a tighter requirement for running at $10^{34} \text{ cm}^{-2}\text{s}^{-1}$, as well as large prescaled samples at $Q^2 < 10 \text{ GeV}^2$. The 10 kHz limit implies that we store 7×10^{10} events per year at the usual LHC assumption of 7×10^6 seconds of operation time per year. We assume an event size of around 100kB, which can be compared with 5Mbytes for ATLAS at the HL-LHC and 20kbytes for ePIC at the EIC. Processor use per event is something like 100 HS06-s, which can be compared with 7000 HS06-s for ATLAS at the HL-LHC at $\mu = 0$, and leads to 7×10^{12} HS06-s per year for data processing. Multiplying this by a factor of 3 to account for Monte Carlo needs, we reach 2×10^{13} HS06 per second, or 7×10^5 MHS06 per year.

Describe the amount and type of resources you expect to need along the timeline of the initiative:

- With resources split into [computing resources | interconnections | facilities | person power required] in the various expected runs/periods.

Based on the scenario introduced above, we estimate:

- Processor resource: 0.7 MHS06;
- Data to tape: 20 PB for each year.

This amounts to about 10–20% of the computing resource required for the ATLAS or CMS experiments before the luminosity upgrade (3-7 MHS06 year for CPU and 200-400 PB/year for tape) [47, 48].

In terms of person-power resources, the LHeC and its data requirements are at the medium-large scale, significantly smaller than ATLAS or CMS. Computing support personnel requirements are thus relatively modest compared with those in place now, or at the HL-LHC.

- Add which external initiatives | events the planning is depending on.

The continued operation of the WLCG is assumed. More detailed considerations have yet to be made.

Furthermore, specific input on the software tools and environment should be provided in meaningful detail:

- Use and/or design of specific software tools for diverse required activities.

Nothing specific to the LHeC is assumed. Object reconstruction software follows on from the advances of the current LHC experiments. Tracking reconstruction, jets, leptons, missing transverse momentum reconstruction and identification can all use standard tools, with simplifications due to the lack of large pile-up. A software infrastructure similar to that of ATLAS would be more than adequate.

- A special emphasis should be provided on the envisaged role of the AI/ML tools in these use-cases.

Once again, the challenges here are not particularly specific to the LHeC, but we would benefit from the progress currently being made in the context of other experiments, and we assume that software experts currently engaged in (HL)-LHC experiments will move on to contribute to the LHeC, hence importing technological developments. One exciting possibility would be to implement a global reconstruction algorithm based on graph-NN to identify b- and c-jets, tau leptons and other jets, similar to the particle flow approach in CMS and the progress being made in ATLAS for the HL-LHC.

- A special emphasis on the external (commercial) software requirements should be provided (e.g. virtualization tools, storage solutions, database solutions).

Given the relatively early stage of the project, these aspects have yet to be considered.

- What type of collaboration you think the software tool development would need between different institutions.

The WLCG framework currently in place for the LHC and HL-LHC would be more than sufficient.

References

- [1] F. Ahmadova et al. The Large Hadron electron Collider as a bridge project for CERN. 3 2025.
- [2] J. de Blas et al. Higgs Boson Studies at Future Particle Colliders. *JHEP*, 01:139, 2020.
- [3] Jorge de Blas, Yong Du, Christophe Grojean, Jiayin Gu, Victor Miralles, Michael E. Peskin, Junping Tian, Marcel Vos, and Eleni Vryonidou. Global SMEFT Fits at Future Colliders. In *Snowmass 2021*, 6 2022.
- [4] Eugenia Celada, Tommaso Giani, Jaco ter Hoeve, Luca Mantani, Juan Rojo, Alejo N. Rossia, Marion O. A. Thomas, and Eleni Vryonidou. Mapping the SMEFT at high-energy colliders: from LEP and the (HL-)LHC to the FCC-ee. *JHEP*, 09:091, 2024.
- [5] Jaco ter Hoeve, Giacomo Magni, Juan Rojo, Alejo N. Rossia, and Eleni Vryonidou. The automation of SMEFT-assisted constraints on UV-complete models. *JHEP*, 01:179, 2024.
- [6] Tommaso Giani, Giacomo Magni, and Juan Rojo. SMEFiT: a flexible toolbox for global interpretations of particle physics data with effective field theories. *Eur. Phys. J. C*, 83(5):393, 2023.
- [7] Jacob J. Ethier, Giacomo Magni, Fabio Maltoni, Luca Mantani, Emanuele R. Nocera, Juan Rojo, Emma Slade, Eleni Vryonidou, and Cen Zhang. Combined SMEFT interpretation of Higgs, diboson, and top quark data from the LHC. *JHEP*, 11:089, 2021.
- [8] P. Agostini et al. The Large Hadron–Electron Collider at the HL-LHC. *J. Phys. G*, 48(11):110501, 2021.
- [9] Ruibo Li, Xiao-Min Shen, Bo-Wen Wang, Kai Wang, and Guohuai Zhu. Probing the trilinear Higgs boson self-coupling via single Higgs production at the LHeC. *Phys. Rev. D*, 101(7):075036, 2020.
- [10] Baradhvaj Coleppa, Mukesh Kumar, Satendra Kumar, and Bruce Mellado. Measuring CP nature of top-Higgs couplings at the future Large Hadron electron collider. *Phys. Lett. B*, 770:335–341, 2017.
- [11] Daniel Britzger, Max Klein, and Hubert Spiesberger. Electroweak physics in inclusive deep inelastic scattering at the LHeC. *Eur. Phys. J. C*, 80(9):831, 2020.
- [12] Jens Erler and Michael J. Ramsey-Musolf. The Weak mixing angle at low energies. *Phys. Rev. D*, 72:073003, 2005.
- [13] Jens Erler and Rodolfo Ferro-Hernández. Weak Mixing Angle in the Thomson Limit. *JHEP*, 03:196, 2018.
- [14] Radja Boughezal, Alexander Emmert, Tyler Kutz, Sonny Mantry, Michael Nycz, Frank Petriello, Kağan Şimşek, Daniel Wiegand, and Xiaochao Zheng. Neutral-current electroweak physics and SMEFT studies at the EIC. *Phys. Rev. D*, 106(1):016006, 2022.
- [15] Matteo Cadeddu, Nicola Cargioli, Jens Erler, Mikhail Gorchtein, Jorge Piekarewicz, Xavier Roca-Maza, and Hubert Spiesberger. Simultaneous extraction of the weak radius and the weak mixing angle from parity-violating electron scattering on C12. *Phys. Rev. C*, 110(3):035501, 2024.
- [16] S. Schael et al. Precision electroweak measurements on the Z resonance. *Phys. Rept.*, 427:257–454, 2006.

- [17] V. M. Abazov et al. Measurement of $\sin^2 \theta_{\text{eff}}^\ell$ and Z -light quark couplings using the forward-backward charge asymmetry in $p\bar{p} \rightarrow Z/\gamma^* \rightarrow e^+e^-$ events with $\mathcal{L} = 5.0 \text{ fb}^{-1}$ at $\sqrt{s} = 1.96 \text{ TeV}$. *Phys. Rev. D*, 84:012007, 2011.
- [18] V. Andreev et al. Determination of electroweak parameters in polarised deep-inelastic scattering at HERA. *Eur. Phys. J. C*, 78(9):777, 2018.
- [19] Chiara Bissolotti, Radja Boughezal, and Kaan Simsek. SMEFT probes in future precision DIS experiments. *Phys. Rev. D*, 108(7):075007, 2023.
- [20] John Ellis, Maeve Madigan, Ken Mimasu, Veronica Sanz, and Tevong You. Top, Higgs, Diboson and Electroweak Fit to the Standard Model Effective Field Theory. *JHEP*, 04:279, 2021.
- [21] Laurent Forthomme, Hamzeh Khanpour, Krzysztof Piotrzkowski, and Yuji Yamazaki. "High energy $\gamma\gamma$ interactions at the LHeC". *PoS, ICHEP2024*:329, 2025.
- [22] Antonio O. Bouzas and F. Larios. Probing $tt\gamma$ and ttZ couplings at the LHeC. *Phys. Rev. D*, 88(9):094007, 2013.
- [23] Hao Sun. Measuring the CKM matrix element V_{td} and V_{ts} at the electron proton colliders. *PoS, DIS2018*:167, 2018.
- [24] Edier Paredes Cruz, Antonio O. Bouzas, and F. Larios. Probing $|V_{td}|$ in single-top production at pe^\mp colliders. *Eur. Phys. J. Plus*, 140(2):130, 2025.
- [25] S. Navas et al. Review of particle physics. *Phys. Rev. D*, 110(3):030001, 2024.
- [26] Fazila Ahmadova et al. Precise Determination of the Strong Coupling Constant from Dijet Cross Sections up to the Multi-TeV Range. 12 2024.
- [27] D. d'Enterria et al. The strong coupling constant: state of the art and the decade ahead. *J. Phys. G*, 51(9):090501, 2024.
- [28] Andrea Dainese, Michelangelo Mangano, Andreas B. Meyer, Aleandro Nisati, Gavin Salam, and Mika Anton Vesterinen, editors. *Report on the Physics at the HL-LHC, and Perspectives for the HE-LHC*, volume 7/2019 of *CERN Yellow Reports: Monographs*. CERN, Geneva, Switzerland, 2019.
- [29] Michał Czakon, Felix Eschment, Marco Niggetiedt, Rene Poncelet, and Tom Schellenberger. Top-Bottom Interference Contribution to Fully Inclusive Higgs Production. *Phys. Rev. Lett.*, 132(21):211902, 2024.
- [30] Michał Czakon, Felix Eschment, Marco Niggetiedt, Rene Poncelet, and Tom Schellenberger. Quark mass effects in Higgs production. *JHEP*, 10:210, 2024.
- [31] Marco Bonetti, Erik Panzer, Vladimir A. Smirnov, and Lorenzo Tancredi. Two-loop mixed QCD-EW corrections to $gg \rightarrow Hg$. *JHEP*, 11:045, 2020.
- [32] Marco Bonetti, Erik Panzer, and Lorenzo Tancredi. Two-loop mixed QCD-EW corrections to $q\bar{q} \rightarrow Hg$, $qg \rightarrow Hq$, and $\bar{q}g \rightarrow H\bar{q}$. *JHEP*, 06:115, 2022.
- [33] Richard D. Ball et al. The PDF4LHC21 combination of global PDF fits for the LHC Run III. *J. Phys. G*, 49(8):080501, 2022.
- [34] S. Alekhin, J. Blümlein, S. Moch, and R. Placakyte. Parton distribution functions, α_s , and heavy-quark masses for LHC Run II. *Phys. Rev. D*, 96(1):014011, 2017.
- [35] Tie-Jiun Hou et al. New CTEQ global analysis of quantum chromodynamics with high-precision data from the LHC. *Phys. Rev. D*, 103(1):014013, 2021.
- [36] S. Bailey, T. Cridge, L. A. Harland-Lang, A. D. Martin, and R. S. Thorne. Parton distributions from LHC, HERA, Tevatron and fixed target data: MSHT20 PDFs. *Eur. Phys. J. C*, 81(4):341, 2021.
- [37] Richard D. Ball et al. The path to proton structure at 1% accuracy. *Eur. Phys. J. C*, 82(5):428, 2022.

- [38] Ilkka Helenius, Marina Walt, and Werner Vogelsang. NNLO nuclear parton distribution functions with electroweak-boson production data from the LHC. *Phys. Rev. D*, 105(9):094031, 2022.
- [39] R. Abdul Khalek et al. Science Requirements and Detector Concepts for the Electron-Ion Collider: EIC Yellow Report. *Nucl. Phys. A*, 1026:122447, 2022.
- [40] J. L. Abelleira Fernandez et al. A Large Hadron Electron Collider at CERN: Report on the Physics and Design Concepts for Machine and Detector. *J. Phys. G*, 39:075001, 2012.
- [41] Chong-Xing Yue, Han Wang, Xue-Jia Cheng, and Yue-Qi Wang. Sensitivity of the future e^-p collider to the coupling of axionlike particles with vector bosons. *Phys. Rev. D*, 107(11):115025, 2023.
- [42] Stefan Antusch, Oliver Fischer, and A. Hammad. Lepton-Trijet and Displaced Vertex Searches for Heavy Neutrinos at Future Electron-Proton Colliders. *JHEP*, 03:110, 2020.
- [43] Georges Aad et al. Search for heavy neutral leptons in decays of W bosons produced in 13 TeV pp collisions using prompt and displaced signatures with the ATLAS detector. *JHEP*, 10:265, 2019.
- [44] Stefan Antusch, Eros Cazzato, and Oliver Fischer. Sterile neutrino searches via displaced vertices at LHCb. *Phys. Lett. B*, 774:114–118, 2017.
- [45] P. Abreu et al. Search for neutral heavy leptons produced in Z decays. *Z. Phys. C*, 74:57–71, 1997. [Erratum: *Z.Phys.C* 75, 580 (1997)].
- [46] J. Adam et al. New constraint on the existence of the $\mu^+ \rightarrow e^+\gamma$ decay. *Phys. Rev. Lett.*, 110:201801, 2013.
- [47] ATLAS Collaboration. ATLAS Software and Computing HL-HLC Roadmap, February 2022.
- [48] CMS Collaboration. CMS Phase-2 Computing Model: Update Document, July 2022.